

1 **Northeast Colorado Extreme Rains Interpreted in a Climate Change Context**

2 Martin Hoerling, Klaus Wolter, Judith Perlwitz, Xiaowei Quan, Jon Eischeid, Hailan Wang,
3 Siegfried Schubert, Henry Diaz, Randall Dole

4 **AFFILIATIONS:** HOERLING, DOLE — NOAA Earth System Research Laboratory, Boulder CO;
5 WOLTER, PERLWITZ, QUAN, EISCHEID, DIAZ—University of Colorado, Cooperative Institute for
6 Research in Environmental Sciences, Boulder CO; SCHUBERT, WANG—NASA Goddard
7 Space Flight Center/GMAO, Greenbelt, MD.

8

9

10 **Summary:** *The probability for an extreme five-day September rainfall event over*
11 *northeast Colorado, as was observed in early September 2013, has likely decreased due*
12 *to climate change.*

13

14

15

16

17

18

19

20

21

22

23

24

25

26 **1. Introduction**

27 Welcome rains over northeast Colorado starting on 9 September 2013 turned into a deluge
28 during 11 September and continued through 15 September. Boulder, an epicenter of this
29 regional event (http://www.crh.noaa.gov/bou/?n=stormtotals_092013), almost doubled its
30 daily rainfall record (from 12.2 cm in July 1919 to 23.1 cm on 12 September 2013), with 43.6 cm
31 for the week. Widespread flooding took 10 lives and caused at least \$2 billion in property
32 damage, second only to the June 1965 floods of eastern Colorado
33 ([http://www.reuters.com/article/2013/09/19/us-usa-colorado-flooding-](http://www.reuters.com/article/2013/09/19/us-usa-colorado-flooding-idUSBRE98H1BA20130919)
34 [idUSBRE98H1BA20130919](http://www.reuters.com/article/2013/09/19/us-usa-colorado-flooding-idUSBRE98H1BA20130919)).

35 Events of similar magnitude are not unprecedented during summer in the Colorado Front
36 Range (Hansen et al. 1978; McKee et al. 1997). Some reach that size in a few hours and are
37 more localized (e.g., Big Thompson in late July 1976), while others take longer and have larger
38 footprints as in June 1965 and September 1938. Interestingly, attributes of the 2013 event
39 including its late-summer occurrence, regional scale, long duration, and slowly changing
40 atmospheric circulation (see Gochis et al. 2014) that transported extreme moisture into the
41 Front Range also characterized the 1938 event.

42 Does the recent occurrence of this extreme event indicate that its likelihood has
43 increased due to global warming? Globally, the atmosphere has become warmer and
44 moister, with the observed rate of increase since the 1970s broadly consistent with that
45 expected from the Clausius–Clapeyron relation (~7% per °C; Hartmann et al. 2013).

46 Heavy precipitation events have increased over much of the United States since 1901,
47 however, with no significant long-term trends over the northern Great Plains or
48 Southwest (Kunkel et al. 2013). Further, the relationship between heavy precipitation
49 and atmospheric water vapor varies seasonally, with moisture availability rather than
50 moisture-holding capacity being a more dominant factor in summer than winter (Berg et
51 al. 2009). Thus, the answer to our question cannot be readily gleaned from globally and
52 annually averaged statistics but requires careful consideration of place and time.

53

54 **2. Datasets and methods**

55 The Global Daily Climatology Data (GDCN; Klein Tank et al. 2002) of station observations
56 is used to create a gridded daily analysis at 1° resolution for 1901–2013. Daily column
57 precipitable water (PW) is based on the National Centers for Environmental Prediction–
58 National Center for Atmospheric Research (NCEP–NCAR) reanalysis product for 1948–
59 2013 (Kalnay et al. 1996).

60 Climate simulations using NASA’s Goddard Earth Observing System (GEOS-5)
61 atmosphere model are diagnosed to determine the effect of time varying forcing on the
62 region’s five-day averaged precipitation and PW. The GEOS-5 model (Rienecker et al.
63 2008, Molod et al. 2012) employs finite-volume dynamics and moist physics as
64 described in Bacmeister et al. (2006). The simulations consist of 12 ensemble members,
65 forced with observed monthly SST, sea ice, and time-varying greenhouse gases for the

66 period 1871–2013 (Schubert et al. 2014). The model was run at 1° horizontal resolution
67 with 72 hybrid-sigma vertical levels.

68 The 1° gridded daily observational and model data are spatially averaged over the
69 northeast Colorado study region (Fig. 1, box), and they are used to calculate running
70 five-day precipitation and PW for September. A region larger than the scale of the event
71 was selected in part to accommodate model capabilities but also to avoid selection bias.
72 Nonetheless, the 2013 heavy rainfall event was large in spatial scale. Weather
73 predictability of the event per se is not addressed herein (see Hamill 2014), but rather
74 how climate change may have affected the relative likelihood of heavy precipitation in
75 this large region. For this purpose, the modeled statistics of heavy five-day rainfall of the
76 recent 30-year period (1983–2012) are compared to that of the last 30 years of the 19th
77 century.

78

79 **3. Results**

80 ***a. Model suitability***

81 The footprint of 2013 rains (Fig. 1a) was partly organized by the Continental Divide and
82 the elevation gain from the Great Plains—topographic features pronounced enough to
83 be captured at 1° resolution in GEOS-5, even though smaller scale aspects of the Front
84 Range terrain are not resolved. The rains were also linked to an abundance of
85 atmospheric water vapor in early September 2013 (Fig. 1b, blue shading) that was

86 transported principally from source regions over the southern Great Plains and Gulf
87 Coast as implied by the anomalous 700-hPa winds superposed on climatological PW (Fig.
88 1b). Such large-scale PW sources are also realistically simulated in GEOS-5, whose
89 climatology includes a strong gradient separating dry west-central Colorado air from
90 moist air over the Great Plains and Gulf of California (c.f., Fig. 1b,d). Most importantly,
91 GEOS-5 generates realistic statistics of five-day September rainfall over the case study
92 region. First, the frequency distribution describing the observed statistics (Fig. 1c, red
93 curve) lies within the spread of curves summarizing the five-day rainfall statistics for the
94 12 model simulations. Second, the statistics of tail events, estimated from 100-year
95 block maxima for any consecutive five-day rainfall total averaged over our northeast
96 Colorado study region, indicate that the model's tail behavior is quite realistic (Fig. 1c,
97 inset). The 2013 event is a rare occurrence relative to both model and observed tail
98 behavior, though the model does generate a few stronger cases in its historical
99 simulation.

100

101 ***b. Simulated long-term change***

102 The ensemble averaged GEOS-5 simulations for September 2013 do not reproduce the
103 observed conditions for either the regional precipitation or PW anomalies (c.f., Fig. 1b,d).
104 The results can be interpreted to indicate that the specific SST/sea ice boundary forcing
105 and greenhouse gas forcings were not the primary drivers, implying a substantial
106 random component of the event itself. Perhaps model biases were related to its failure

107 to simulate the 2013 event such as an inability to depict the particular pattern of
108 atmospheric circulation and its interaction with complex topography. Yet, this must be
109 weighed against the realistic characterization of the statistics of extreme rainfall events
110 over northeast Colorado (Fig. 1c). Ultimately, further analysis using other climate
111 models will be required to clarify these issues.

112 Nonetheless, the absence of such events in the 12-member September 2013 simulations
113 neither affirms nor refutes a possible effect of long-term change on event likelihood or
114 intensity. To address this issue, we compare five-day rainfall statistics over northeast
115 Colorado between two 30-year periods: one for 1983–2012 that is representative of
116 current climate and the other for 1871–1900 that is representative of preindustrial
117 climate. The model produces realistic global changes between these periods that
118 compare well with observations—global land surface temperature rises 0.9°C (Fig. 2a)
119 and global PW rises 5.7% (Fig. 2b).

120 Despite a warmer and moister climate, the frequency of September heavy five-day rain
121 events does not increase in the simulations but substantially declines in northeast
122 Colorado (Fig. 2c). Using the model's 95th percentile of five-day rainfall totals, we find a
123 12% decline in occurrence during recent decades compared to the late 19th century.
124 Using the model's 99th percentile, we find a 44% decline in frequency. The simulated
125 magnitude of September heavy five-day rainfall over northeast Colorado also declines.
126 For the 99th percentile, the threshold value falls from 49 mm in the late 19th century to
127 45 mm in the recent period.

128

129

130 ***c. Conditioning of heavy five-day rain events***

131 To understand the above results we examine the relationship between the probability
132 of heavy five-day rainfall and atmospheric water vapor. Statistics of five-day rainfall are
133 examined for the lower and upper decile of five-day PW (Fig. 2e). For dry atmospheric
134 conditions (red curve), very few rainfall occurrences exceed 35 mm (95th percentile)
135 and none exceed 50 mm (99th percentile). For wet atmospheric conditions (black curve),
136 the full range of five-day rainfall amounts is possible. Thus, though a necessary
137 condition for extreme rainfall, high atmospheric water vapor is not sufficient.

138 Even though the simulated long-term increase in PW over northeast Colorado is small in
139 magnitude (~6%), high five-day PW events increase in frequency (Fig. 2d). One would
140 thus expect to also witness an increase rather than a decrease in heavy rain event
141 probabilities over the region in GEOS-5. The contrary behavior suggests changes in other
142 climate features (e.g., atmospheric circulation and vertical stability) act to counter the
143 increase in water vapor over the region in the model.

144

145 **4. Conclusion**

146 Our analysis of the GEOS-5 simulations leads to a diagnosis that the occurrence of
147 extreme five-day rainfall over northeast Colorado during September 2013 was not made

148 more likely, or more intense, by the effects of climate change. From an observational
149 perspective, analogous events have occurred before in the Front Range, perhaps most
150 strikingly similar in September 1938, long before appreciable climate change.

151 Although our model results suggest that the occurrence of this recent extreme has
152 become less probable over northeast Colorado due to climate change, model
153 projections do show an increase in the intensity of maximum five-day precipitation over
154 the globe and for annual averages as a whole by the end of the 21st century (Sillman et
155 al. 2013). Yet, a slight decline in intensity of the maximum five-day precipitation over
156 the central Great Plains during summer is also projected (Sillman et al. 2013),
157 emphasizing that global and annual perspectives of climate change may not always
158 pertain to events at a specific place and time.

159 A strength of our study is the availability of an ensemble of long-term climate
160 simulations spanning 1871–2013, conducted at 1° spatial resolution, that permits an
161 analysis of statistical properties of the change in extreme events. For the purpose of
162 studying regional five-day rainfall events over northeast Colorado, the GEOS-5 model
163 has the attribute of realistically characterizing the tails of the distribution. A weakness of
164 our study is that results are based on a single model and thus require confirmation using
165 additional models. Also, the physical reasons for the decline in simulated frequency of
166 extreme five-day rainfall over northeast Colorado during September are not addressed.
167 Better understanding of the delivery mechanisms for atmospheric moisture that

168 produce heavy rain events and how those mechanisms respond to global warming will
169 be critical.

170

171

172 **References**

173 Bacmeister, Julio T., Max J. Suarez, Franklin R. Robertson, 2006: Rain Reevaporation,
174 Boundary Layer–Convection Interactions, and Pacific Rainfall Patterns in an AGCM. *J.*
175 *Atmos. Sci.*, **63**, 3383–3403.

176 Berg, P., J. Haerter, P. Thejll, C. Piani, S. Hagemann, and J. Christensen, 2009: Seasonal
177 characteristics of the relationship between daily precipitation intensity and surface
178 temperature. *J. Geophys. Res.*, **114**, D18102, doi:10.1029/2009JD012008.

179 Daly, C., Halbleib, M., Smith, J.I., Gibson, W.P., Doggett, M.K., Taylor, G.H., Curtis, J., and
180 Pasteris, P.A. 2008. Physiographically-sensitive mapping of temperature and
181 precipitation across the conterminous United States. *International Journal of*
182 *Climatology*, 28: 2031-2064.

183 Gochis, D., and Coauthors, 2014: The Great Colorado Flood of September 2013. *Bull. Amer. Met.*
184 *Soc.*, submitted.

185 Hamill, T., 2014: Performance of Operational Model Precipitation Forecast
186 Guidance During the 2013 Colorado Front-Range Floods. *Mon. Wea. Rev.*

187 doi:10.1175/MWR-D-14-00007.1, in press.

188

189 Hansen, W.R., B.J. Chonic, and J. Matelock, John, 1978: Climatography of the Front Range
190 urban corridor and vicinity, Colorado. USGS. Professional Paper 1019, 59pp. (available at:
191 <http://pubs.usgs.gov/pp/1019/report.pdf>)

192 Hartmann, D.L., A.M.G. Klein Tank, M. Rusticucci, L.V. Alexander, S. Brönnimann, Y.
193 Charabi, F.J. Dentener, E.J. Dlugokencky, D.R. Easterling, A. Kaplan, B.J. Soden, P.W.
194 Thorne, M. Wild and P.M. Zhai, 2013: Observations: Atmosphere and Surface. In:
195 *Climate Change 2013: The Physical Science Basis. Contribution of Working Group I to the*
196 *Fifth Assessment Report of the Intergovernmental Panel on Climate Change* [Stocker,
197 T.F., D. Qin, G.-K. Plattner, M. Tignor, S.K. Allen, J. Boschung, A. Nauels, Y. Xia, V. Bex and
198 P.M. Midgley (eds.)]. Cambridge University Press, Cambridge, United Kingdom and New
199 York, NY, USA.

200 Kalnay, E., and Coauthors, 1996: The NMC/NCAR 40-Year Reanalysis Project. *Bull. Amer.*
201 *Meteor. Soc.*, 77, 437-471.

202 Klein Tank, A.M.G., and Coauthors, 2002: Daily dataset of 20th century surface air
203 temperature. *Int. J. Climatol.*, 22, 1441-1453.

204 Kunkel, K., and Coauthors, 2013: Monitoring and understanding trends in extreme
205 storms. State of Knowledge. *Bull. Amer. Met. Soc.*, 499-514, doi:10.1175/BAMS-D-11-
206 00262.1

207 McKee, T.B., and N.J. Doesken, 1997: Colorado Extreme Storm Precipitation Data Study. Final
208 Report. Colorado Climate Center, Colorado State University, Fort Collins, CO, 109pp. (available
209 at: http://climate.colostate.edu/pdfs/Climo_97-1_Extreme_ppt.pdf)

210 Molod, A., L. Takacs, M. Suarez, J. Bacmeister, I.-S. Song, and A. Eichmann, 2012. The
211 GEOS-5 Atmospheric General Circulation Model: Mean Climate and Development from
212 MERRA to Fortuna. *NASA Technical Report Series on Global Modeling and Data*
213 *Assimilation, NASA TM—2012-104606*, Vol. **28**, 117 pp.

214 Rienecker, M. M., and Coauthors, 2008: The GEOS-5 data assimilation system—
215 Documentation of versions 5.0.1, 5.1.0, and 5.2.0. NASA Tech. Rep. Series on Global
216 Modeling and Data Assimilation, NASA/TM-2007-104606, Vol. 27, 95 pp.

217 Schubert, S., H. Wang, R. Koster, M. Suarez, and P. Groisman, 2014: Northern Eurasian
218 heat waves and droughts . *J. Climate*, doi:10.1175/JCLI-D-13-00360.1, in press.

219 Sillman, J., V. Kaharin, F. Zweirs, X. Zhang, and D. Bronaugh, 2013: Climate extreme
220 indices in the CMIP5 multimodel ensemble: Part 2. Future climate projections. *J.*
221 *Geophys. Res.* , **118**, 2473-2493, doi:10.1002/jgrd.50188.

222

223

224

225

226

227

228

229

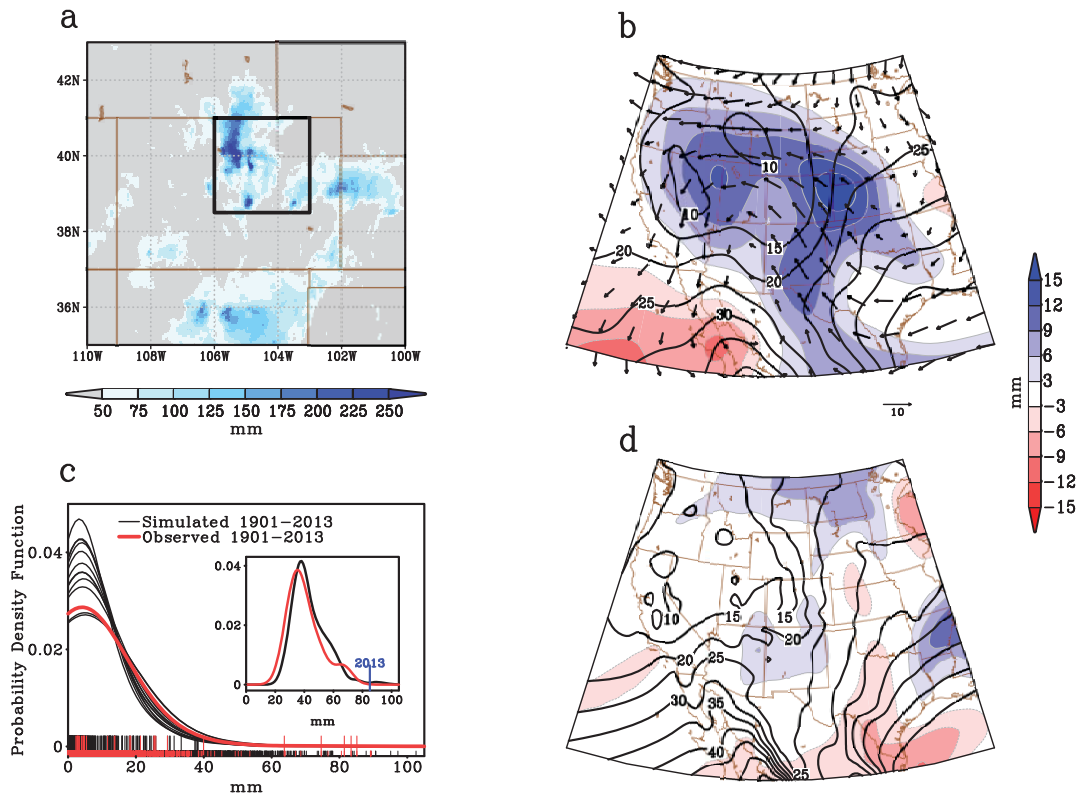
230

231 **Figure Captions**

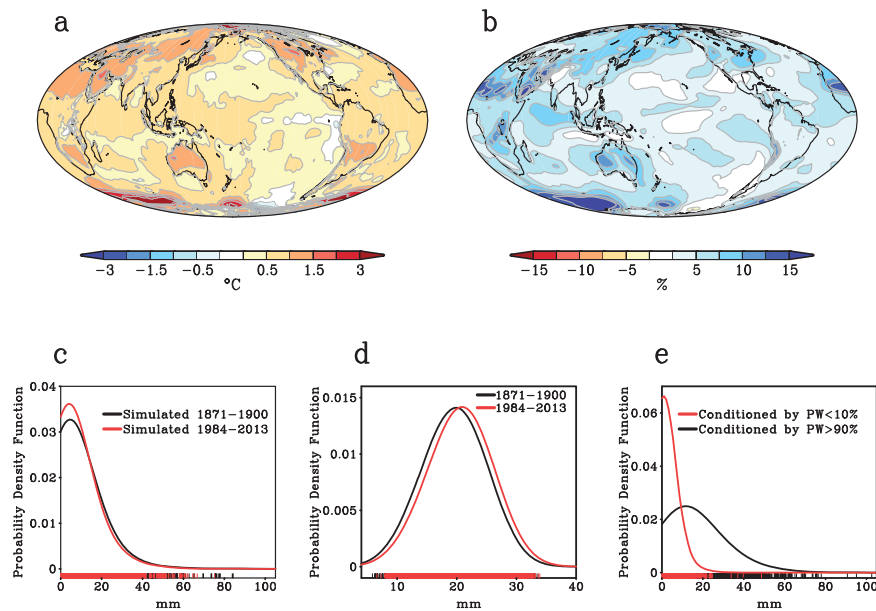
232 **Figure 1.** a) Observed five-day cumulative precipitation totals during September 10-14,
233 2013, for Colorado and neighboring states at the peak of the extreme event. The box
234 outline denotes the northeast Colorado domain of most extreme precipitation with
235 estimated 84mm five-day precipitation. b) Observed five-day average column
236 precipitable water (PW) for the period September 10-14, 2013. Shaded values are
237 departures from a 1948-2013 reference period; the overlain contours indicate the
238 reference period climatology for that 5-day period, overlain arrows are 700 hPa wind
239 anomalies. (Data source: NCEP/NCAR Reanalysis) c) Frequency distributions (PDFs) of
240 five-day cumulative precipitation during September averaged over the study area shown
241 in Fig 1a for observation (red curve, 3390 values) and for individual ensemble members
242 of climate model simulations (black curves, 3390 values per simulation, 51480 total) for
243 the period 1901-2013. Individual 5-day running totals are shown with tick marks, and
244 the September 2013 values are indicated with taller tick marks. The PDFs are non-
245 parametric curves utilizing kernel density estimation and a Gaussian smoother. Inset
246 shows the frequency distribution of 100-year block maximum values of the wettest 5-
247 day rainfall for all consecutive five-day periods in September based on observations
248 (red; 30 samples), and the ensemble of GEOS-5 simulations (black; 360 samples) for the
249 100-year period 1913-2012. Observed 5-day peak value in September 2013 shown by
250 blue tick mark. d) As in Figure 1b but for the GEOS5 climate simulations. The simulated
251 departures (shades) are based on the 12-member ensemble mean, and are computed
252 relative to the model climatology (contours).

253 **Figure 2.** a) Simulated long-term change in September monthly averaged surface
254 temperature displayed as the difference between 1984-2013 and 1871-1900. b) As in
255 Fig 2a but for the simulated change in September monthly averaged PW expressed as %
256 change of the 1871-1900 reference. c) Climate model simulated frequency distributions
257 of five-day September precipitation totals (mm) over the study area for 1871-1900
258 (black curve) and the 1984-2013 (red curve) period utilizing twelve GEOS5 model
259 simulations (10800 values). Tick marks indicate individual samples. d) As in Fig. 2c but
260 for five-day September PW for 1871-1900 (black) and 1984-2013 (red) 2e. Simulated
261 PDFs of September five-day precipitation totals conditioned by the lowest 10% of PW
262 (red curve, n=5139) and the highest 10% PW (black, n=5195) values.

263



264
 265 **Figure 1.** a) Observed five-day cumulative precipitation totals during September 10-14,
 266 2013, for Colorado and neighboring states at the peak of the extreme event. The box
 267 outline denotes the northeast Colorado domain of most extreme precipitation with
 268 estimated 84mm five-day precipitation. b) Observed five-day average column
 269 precipitable water (PW) for the period September 10-14, 2013. Shaded values are
 270 departures from a 1948-2013 reference period; the overlain contours indicate the
 271 reference period climatology for that 5-day period, overlain arrows are 700 hPa wind
 272 anomalies. (Data source: NCEP/NCAR Reanalysis) c) Frequency distributions (PDFs) of
 273 five-day cumulative precipitation during September averaged over the study area shown
 274 in Fig 1a for observation (red curve, 3390 values) and for individual ensemble members
 275 of climate model simulations (black curves, 3390 values per simulation, 51480 total)
 276 for the period 1901-2013. Individual 5-day running totals are shown with tick marks, and
 277 the September 2013 values are indicated with taller tick marks. The PDFs are non-
 278 parametric curves utilizing kernel density estimation and a Gaussian smoother. Inset
 279 shows the frequency distribution of 100-year block maximum values of the wettest 5-
 280 day rainfall for all consecutive five-day periods in September based on observations (red;
 281 30 samples), and the ensemble of GEOS-5 simulations (black; 360 samples) for the 100-
 282 year period 1913-2012. Observed 5-day peak value in September 2013 shown by blue
 283 tick mark. d) As in Figure 1b but for the GEOS5 climate simulations. The simulated
 284 departures (shades) are based on the 12-member ensemble mean, and are computed
 285 relative to the model climatology (contours).



287

288 **Figure 2.** a) Simulated long-term change in September monthly averaged surface
 289 temperature displayed as the difference between 1984-2013 and 1871-1900. b) As in
 290 Fig 2a but for the simulated change in September monthly averaged PW expressed as %
 291 change of the 1871-1900 reference. c) Climate model simulated frequency distributions
 292 of five-day September precipitation totals (mm) over the study area for 1871-1900
 293 (black curve) and the 1984-2013 (red curve) period utilizing twelve GEOS5 model
 294 simulations (10800 values). Tick marks indicate individual samples. d) As in Fig. 2c but
 295 for five-day September PW for 1871-1900 (black) and 1984-2013 (red) 2e. Simulated
 296 PDFs of September five-day precipitation totals conditioned by the lowest 10% of PW
 297 (red curve, n=5139) and the highest 10% PW (black, n=5195) values.